X-ray induced secondary particle counting with thin NbTiN nanowire superconducting detector

Branny, Artur; Didier, Pierre; Zichi, Julien; Zahed, Iman Esmaeil; Steinhauer, Stephan; Zwiller, Val; Vogt, Ulrich

DOI
10.1109/TASC.2021.3066578

Publication date
2021

Document Version
Final published version

Published in
IEEE Transactions on Applied Superconductivity

X-ray induced secondary particle counting with thin NbTiN nanowire superconducting detector

Art Branny, Pierre Didier, Julien Zichi, Iman E. Zadeh, Stephan Steinhauer, Val Zwiller, and Ulrich Vogt

***Abstract*—We characterized the performance of a biased superconducting nanowire to detect X-ray photons. The device, made of a 10 nm thin NbTiN film and fabricated on a dielectric substrate (SiO_2, Nb_3O_5) detected 1000 times larger signal than anticipated from direct X-ray absorption. We attributed this effect to X-ray induced generation of secondary particles in the substrate. The enhancement corresponds to an increase in the flux by the factor of 3.6, relative to a state-of-the-art commercial X-ray silicon drift detector. The detector exhibited 8.25 ns temporal recovery time and 82 ps timing resolution, measured using optical photons. Our results emphasise the importance of the substrate in superconducting X-ray single photon detectors.**

***Index Terms*—Superconducting thin film, nanowire single photon detector, X-ray detection, niobium titanium nitride.**

I. Introduction

SUPERCONDUCTING nanowire single-photon detectors (SNSPDs) have reached technological maturity for sensing optical photons that span across the electromagnetic spectrum from the visible to the near-infrared. In order to obtain highly-desired features such as single photon sensitivity, picosecond-fast timing resolution [1] and near-unity detection efficiency [2], the current scientific interest focuses on extending these capabilities to mid-infrared [3] and X-ray radiation [4]. Higher time resolution and lower detection limits would advance many important applications such as medical computed tomography, solid-state diagnostics and remote sensing. SNSPDs can also cover areas as large as several 100×100 μm^2 and be arranged in a dense pixel array with sub-100 nm footprints and separations. In particular for X-ray detection, such flexibility of fabricating the active area can lead to a new generation of devices with much improved spatial and time resolution for applications such as X-ray phase contrast imaging [5], X-ray spectroscopy [6], and inelastic X-ray scattering [7].

A. Branny, J. Zichi, S. Steinhauer, V. Zwiller, and U. Vogt are with the Department of Applied Physics, KTH Royal Institute of Technology, SE-106 91 Stockholm, Sweden. Corresponding author e-mail: branny@kth.se and zwiller@kth.se

P. Didier is with the Grenoble INP - Phelma, 46 avenue Félix Viallet, 38031 Grenoble Cedex 1, France.

I.E. Zadeh is with Optics Research Group, ImPhys Department, Faculty of Applied Sciences, Delft University of Technology, Delft 2628 CJ, The Netherlands.

We thank Martin Brunzell and Theodor Staffas for their help. We thank Rabia Akan for help with weighing of NbTiN films.

This work was supported by the research fund from the the Knut and Alice Wallenberg Foundation Grant "Quantum Sensors", the Swedish Research Council (VR) through the VR Grant for International Recruitment of Leading Researchers (Ref 2013-7152), and from the European Union's Horizon 2020 Research and Innovation Program (820423, 777222).

Currently, the state-of-the-art photon counting X-ray detectors are based on photon-to-electron conversion facilitated by a biased semiconductor [8], [9]. This technology offers 10 ns timing resolution, several 100s ns of dead times, and count rates up to a million counts per second (Mcps) for a single pixel [10], [11]. In comparison, SNSPD technology with high timing resolution reaching the few ps level, Gcps count rate [12], and single photon sensitivity has a great potential to improve current photon counting X-ray detection schemes.

The first attempt of using superconducting current for detecting X-ray photons dates back to early 1990s [13]. During the past three decades, a range of different materials were implemented. Among them are granular Al [14] and W [15], crystalline NbVN [16], NbN [17], Nb [18], TaN [19], and amorphous WSi [4]. Over the years material and fabrication quality have improved, leading to better and saturated X-ray SNSPDs (X-SNSPD) [19]. The progress towards enhancing the direct X-ray absorption efficiency has been continued by fabricating structures that are thicker, wider and made of heavier elements. For instance, a 100 nm thick and 920 nm wide WSi X-SNSPD was demonstrated to reach few percent absorption efficiency for 6 keV photons [4].

Substrate-mediated X-ray detection is another important and relevant aspect of X-SNSPD devices. As shown in [17], the detection efficiency can be increased through X-ray induced luminescence generated in the substrate. However, the magnitude of this enhancement is not fully quantified. In previous reports, the substrate has been assumed to diminish the spatial and temporal resolution of the detection process, but a limited amount of experimental work in the literature motivates further studies on substrate-mediated X-SNSPDs.

In this work, we introduce thin-film NbTiN SNSPD to X-ray detection and quantify its performance. Our device demonstrates a large enhancement of the total count rate per detection area which we attribute to secondary processes generated in the substrate. Our results shine light on the importance of substrate engineering in further development of superconducting X-ray single photon detectors.

II. Device Fabrication

The first fabrication step of the X-SNSPD was room temperature deposition of a 10 nm thin film of NbTiN in an Ar/N_2 atmosphere by reactive magnetron sputtering using two separate Nb and Ti targets. A detailed description of the setup, fabrication conditions and film's properties, including sheet resistance and critical temperature can be found in [20]. The film was deposited on a dielectric substrate supported by Si

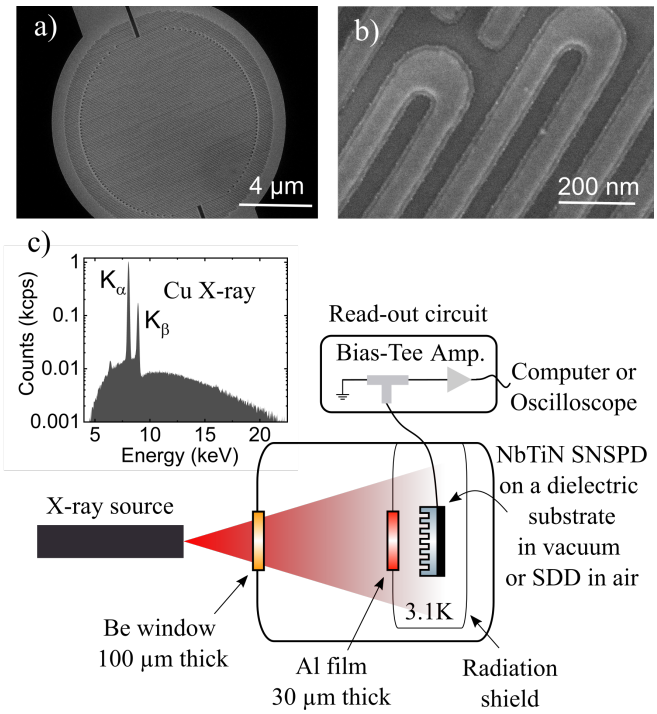

Fig. 1. (a,b) Scanning electron microscope images of the NbTiN detector revealing its structure: circular area with 10 μm diameter, and 0.5 filling factor. (c) A diagram of the experimental setup. A copper X-ray source illuminates the NbTiN superconducting single photon detector (X-SNSPD) that is kept at cryogenic temperature of 3.1 K. The inset shows the corresponding X-ray spectrum.

wafer (0.3 mm thick). The substrate contained a stack of alternating SiO_2 and Nb_2O_5 layers with total thicknesses of 1.1 and 0.6 μm respectively. Fig. 1 a,b show scanning electron microscopy images of a 70 nm wide nanowire detector with 0.5 filling factor and circular area of 10 μm. The structure was defined by a standard procedure involving electron beam lithography, negative resist mask (hydrogen silsesquioxane, HSQ) and subsequent reactive ion etching in SF_6. The evident inner margin feature surrounding the nanowire is due to a layer of mask which was not fully etched away.

III. Experimental Setup

Fig. 1c displays a schematic diagram of the experimental setup. A microfocus X-ray source (Phoenix xs 160T) with Copper (Cu) anode and an acceleration voltage of 30 kV was used to generate a diverging beam of X-ray photons with energies mostly confined to K_α = 8.05 keV and K_β = 8.9 keV lines that constitute 0.60 and 0.13 of the total intensity, respectively. The remaining portion of generated X-ray photons originates from continuous Bremsstrahlung radiation manifested by a broadband emission in the spectrum, as shown in the inset of Fig. 1c. The spectrum was acquired by a photon-counting silicon drift detector (SDD, Amptek X123 with a 100 μm pinhole and 12.5 μm thick Beryllium window) and taken at the same distance from the source as the X-SNSPD. The SDD was also used to measure the total number of X-ray photons arriving at the X-SNSPD. The illuminated X-SNSPD was kept in a vacuum chamber at the pressure and the temperature below 10^{-6} mbar and 3.1 K, respectively. A Beryllium (Be) vacuum window (100 μm thick) and Aluminum (Al) filter (30 μm thick), placed in the line of sight, provided access to the detector. The electrical signal from the X-SNSPD was sent through a 50 Ω coaxial cable to a bias tee and to a commercial driver (Single Quantum Eos) that amplifies, triggers and reads-out detection events. The temporal response of the decaying voltage peak and the timing resolution were measured with an oscilloscope (LeCroy WaveRunner 640 Zi with 4 GHz bandwidth) connected to the driver. The timing resolution was acquired by recording time correlations events between the trigger of a 850 nm 2 ps pulsed laser and the SNSPD signal. Note that all data presented in this work was obtained with the same X-SNSPD device (i.e. with 70 nm wide and 10 nm thick wires).

IV. Results and Discussion

A. Dark count rate and critical current

To characterize the X-SNSPD we measured voltage and count rate as a function of bias current, I_b under no illumination. This allows for quantifying the dark count rates (DCR) and the critical current, I_c. We observe the maximum DCR on the order of 10 kcps and I_c = 19.5 μA which we attribute to fabrication imperfections over a large area and the nanowire's cross-section (i.e. 70 nm wide, 10 nm thick), respectively. Lower DCR values of few cps and below can be achieved in detectors with significantly shorter [21], [22] and wider nanowires [4], [18], [19]. The trade-off of reducing DCR in such ways leads to reduced ability of detecting low-energy particles and the overall detection efficiency.

B. X-ray induced signal

Fig. 2a shows the count rate of X-SNSPD under X-ray illumination superimposed on DCR for different I_b. The signal to noise ratio of one is reached at I_b = 18.9 μA = 0.97 I_c, where the total signal is equal to 500 cps. We consider that secondary emission from Al filter is negligible due to highly divergent x-ray beam, the low probability of generating secondary particles, the large (few cm) distance to the detector, and the small area of the detector. It is evident from Fig. 2a that the increase of the count rate in a region below 18 μA bias current is caused by the X-ray irradiation. The device becomes more sensitive to incoming X-ray photons with increasing I_b without saturating the device. We attribute the non-saturated signal to the nanowire dimensions. All X-SNSPDs that previously have shown saturation [4], [18], [19] were made of thick and wide nanowires (e.g. 100×920 nm). This contrasts with our device that has much smaller dimensions (i.e. 10×70 nm). The smaller the nanowire cross-section the lower the probability of absorbing X-ray photons. The reduction in nanowire cross-section also makes the device more sensitive to detect low-energy particles [3]. Therefore, one potential explanation is that the device mostly detects secondary particles such as electrons, photons, and phonons with low enough energy and momentum for which the detector does not saturate. Observation of non-saturated signal in devices with such small cross-section is consistent with

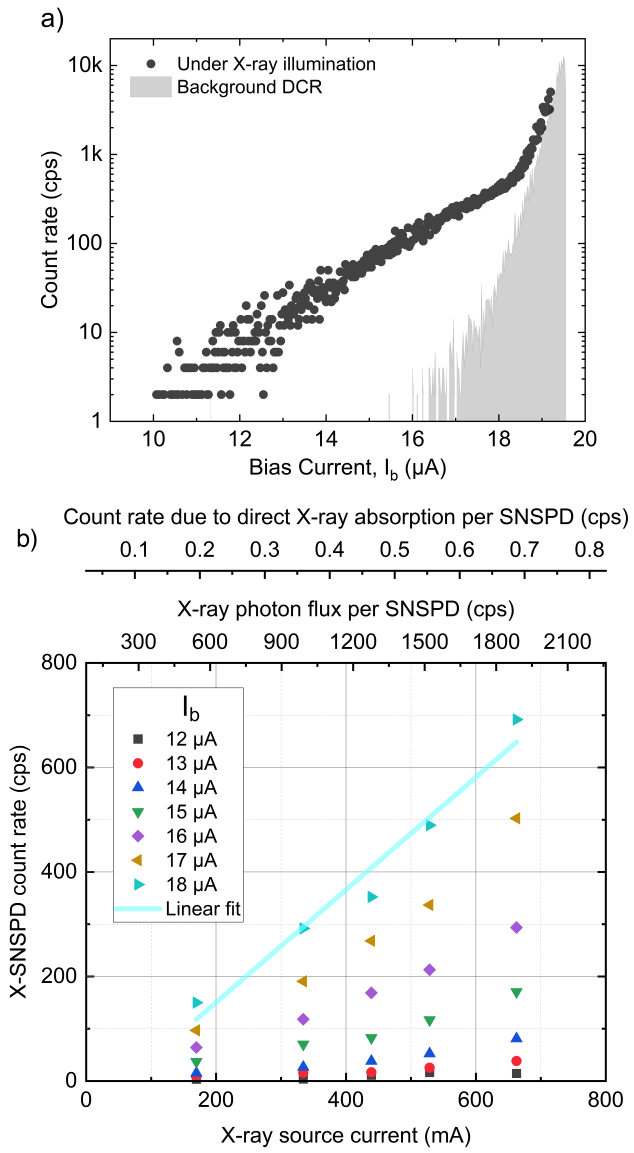

Fig. 2. (a) The count rate of X-SNSPD detection events excluding dark counts as a function the bias current, I_b, shown in semi-logarithmic scale. The X-ray power was 15 W (current = 0.5 mA), the DCR is indicated by the grey underlined area. (b) The rate of X-SNSPD detection events at several X-SNSPD bias currents, from I_b = 12 to 18 μA corresponding to 0.62 and 0.92 of I_c, respectively, as a function of incoming X-ray irradiation, expressed as X-ray source current, X-ray photon flux and direct X-ray absorption. Each data set follows a linear relation.

other report (i.e. 5×120 nm) [17]. The authors of this work attributed this enhancement to secondary particles generated in the substrate. The contribution of secondary particles will be further discussed in the following sections where we consider absorption probability of the film and the device detection efficiency.

C. Device detection efficiency

For a $Nb_{0.86}Ti_{0.14}N$ alloy with a density of ρ = 6.1 g/cm^3, the effective linear attenuation coefficient at 8 keV is $\mu = 7.3\times10^{-5}$ per nm. After accounting for 0.5 fill factor and 10 nm film thickness, the total absorption of the X-SNSPD device becomes 3.63×10^{-4}. To obtain the film density, we measured the weight of a NbTiN film sputtered on a 4 inch wafer. The stoichiometric ratio was determined by X-ray photoelectron spectroscopy [20].

Next, we use the SDD at room temperature and atmospheric pressure to measure the total X-ray flux, the X-SNSPD is under. For 20 W of X-ray power (0.67 mA at 30 kV), the SDD acquires 12.6×10^3 X-rays per second through a 100 μm circular pinhole. This value is the result of integrating the signal between 4-25 keV and including 10% dead time. This raw SDD count rate is decreased by the transmission loss through a 30 cm air gap, that is otherwise in vacuum during X-SNSPD experiments, and the internal loss of the SDD. Therefore, we obtain the total X-ray flux at the X-SNSPD after accounting for these loses. To this end, we calculated the total count rate to be 19.2×10^3 X-rays per second, equivalent to the total flux of 2.44 X-rays per μm^2. This leads to the X-ray intensity at the X-SNSPD to be 191.6 X-rays per second, calculated by multiplying the flux by the X-SNSPD area (a 10 μm circular pinhole). Further we multiply the intensity by the direct X-ray absorption probability of the superconducting film and arrive at the count rate of 0.07 X-rays per second. This anticipated count rate is in the stark contrast with a several 100s of counts recorded by the device (see Fig. 2a). For instance, 700 cps detected by the X-SNSPD is 1000 times larger than the contribution from the direct X-ray absorption. This count rate also leads to the flux of 8.9 cps per μm^2, which is 3.6 times larger than the one obtained with the SDD. This strongly implies that secondary particles constitute a significant majority of the signal.

D. Single particle sensitivity

A common way to assess single particle sensitivity in a counting detector is to measure its count rate as a function of incoming intensity. Fig. 2b displays this relationship for X-SNSPD operating at different bias currents. There, the incoming intensity is presented in three ways as (i) X-ray source current, (ii) X-ray photon flux per SNSPD and (iii) the count rate due to direct X-ray absorption. All sets of data follow a linear trend. As expected, all the slopes increase with the bias current, I_b. The hallmark of single particle sensitivity is a linear fit with slope of one. The linear fit shown in Fig.2b gives different slopes depending on the definition of the incoming intensity. Respectively to the above order the slopes are (i) 1.1, (ii) 0.4, and (iii) 1077. Such large slope in the direct X-ray absorption provides another manifestation that the contribution from secondary particles dominates the signal.

E. Substrate-mediated X-ray detection

The measurement of the total number of X-ray photons arriving at the X-SNSPD implies the efficiency larger than unity if only direct X-ray absorption in the nanowire is considered. Thus, we conclude that secondary particles contribute to the overall count rate. These particles might include softer X-ray photons, optical photons, hot electrons and phonons. We do not eliminate any of these conversion processes. However,

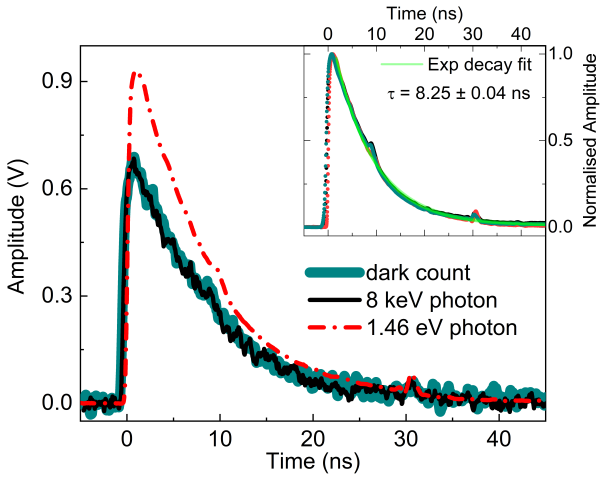

Fig. 3. An electrical pulse generated by a detection event in the X-SNSPD due to a dark count (thick dark cyan solid line), absorption of an optical photon (thin red dot dashed line), and X-ray illumination (thin black solid line). The inset displays normalised pulses for all three detection events fitted with a single exponential decay that exhibit identical characteristic time constant, τ = 8.25 $\pm$ 0.04 ns.

we recognise that the luminescence property of the substrate might produce a significant number of optical photons. In fact, SiO_2 and Nb_3O_5 has been shown to luminesce visible photons (400 nm and 650 nm) due to X-ray irradiation [23], [24]. These optical photons have enough energy to cause detection events in our device. Also, optical transparency of the substrate increases the chances of detecting optical photons that were created outside the detector area. The 1000-fold discrepancy between measured and absorbed number of X-ray photons suggests that a single X-ray photon generates a large number of secondary particles. On the other hand, if one seeks to reduce substrate-mediated contributions, one strategy is to increase the nanowire cross section, as demonstrated in [19]. Another would be to suspend the SNSPD above the substrate. To take this work further we suggest to perform time-resolved correlation measurements which would differentiate direct detection from secondary particles using characteristic decay times. This method would also allow for quantifying the impact of the substrate on the detector's temporal resolution.

F. Voltage signal pulse and temporal response

The detection principle of SNSPDs relies on counting voltage pulses generated by photon-induced superconductor-to-normal transitions. Each count is recorded during the pulse rise time when a predefined and constant voltage threshold is reached. Fig. 3a displays pulses generated in three different cases - due to a random dark count, absorption of an optical photon (1.46 eV, 850 nm) and X-ray illumination (8 keV, 0.155 nm). The height of generated voltage pulses depends on the 50 Ω circuit impedance and the operating bias current, I_b. The normal-to-superconductor recovery of SNSPDs after a detection event, known as dead time, is manifested by an exponential decay. We do not anticipate differences in pulse heights and decay times between the three cases. This is because the decay time is defined by the nanowire's kinetic inductance and the impedance [25], which are invariant to the incoming photon energy. As presented in the inset of Fig. 3a, all detection types exhibit identical exponential decay times τ = 8.25 $\pm$ 0.04 ns. The origin of additional spikes at 10 ns and 32 ns and other pulse signal distortions are due to reflections and impedance mismatches. Please note that difference in pulse heights between optical and X-ray radiation is due to different I_b. Also, during all experiments involving optical photons the X-SNSPD was placed in a different chamber cryostat that provided access for optical fibers.

We also measure temporal resolution of the device using optical photons (1.46 eV, 850 nm) and quantify it as full-width at half-maximum from a Gaussian distribution fitting. The X-SNSPD can detect the arrival of optical photons with resolution equal to Δt = 82.0$\pm$0.6 ps. Note that this jitter was measured with room temperature amplification electronics. To improve the jitter and reach sub-10 ps, one needs to use cryogenic amplifiers and optimised detection electronics [26]. This suggests that under pulsed X-ray irradiation, direct absorption in the X-SNSPD is likely to show ps decay times while any substrate-mediated detection, would be pronounced by a different tine jitter ranging from ps to μs. This makes correlation measurements a great tool in differentiating the origin of detection events.

V. Conclusion

In summary, we introduced thin-film NbTiN superconducting nanowire devices to X-ray detection. We observed that the signal exceeded 1000-fold the direct X-ray absorption of the film. We ascribe this enhancement to substrate-mediated X-ray-to-secondary-particle conversion. We also estimated that our X-SNSPD detects 3.6 times larger flux than a state-of-the-art commercial X-ray SDD. Our results reveal the importance of secondary processes and the substrate in superconducting X-ray single photon detectors. This leads us to conclude that further work on the impact of substrate in X-ray detection has a potential to pave the way towards substrate engineering. This would involve optimising the substrate composition and the nanowire's dimensions for making faster, more sensitive, and more efficient detectors.

References

[1] B. Korzh, Q.-Y. Zhao, J. P. Allmaras, S. Frasca, T. M. Autry, E. A. Bersin, A. D. Beyer, R. M. Briggs, B. Bumble, M. Colangelo, G. M. Crouch, A. E. Dane, T. Gerrits, A. E. Lita, F. Marsili, G. Moody, C. Peña, E. Ramirez, J. D. Rezac, N. Sinclair, M. J. Stevens, A. E. Velasco, V. B. Verma, E. E. Wollman, S. Xie, D. Zhu, P. D. Hale, M. Spiropulu, K. L. Silverman, R. P. Mirin, S. W. Nam, A. G. Kozorezov, M. D. Shaw, and K. K. Berggren, "Demonstration of sub-3 ps temporal resolution with a superconducting nanowire single-photon detector," *Nature Photonics*, vol. 14, no. 4, pp. 250–255, 2020. [Online]. Available: http://www.nature.com/articles/s41566-020-0589-x

[2] F. Marsili, V. B. Verma, J. A. Stern, A. E. Harrington, S. nd Lita, T. Gerrits, I. Vayshenker, B. Baek, M. D. Shaw, R. P. Mirin, and S. W. Nam, "Detecting single infrared photons with 93% system efficiency," *Nature Photonics*, vol. 7, no. 3, pp. 210–214, 2013. [Online]. Available: http://www.nature.com/articles/nphoton.2013.13

[3] F. Marsili, F. Bellei, F. Najafi, A. E. Dane, E. A. Dauler, R. J. Molnar, and K. K. Berggren, "Efficient single photon detection from 500 nm to 5 μm wavelength," *Nano Letters*, vol. 12, no. 9, pp. 4799–4804, 2012. [Online]. Available: http://pubs.acs.org/doi/10.1021/nl302245n

[4] X. Zhang, Q. Wang, and A. Schilling, "Superconducting single x-ray photon detector based on w $_{0.8}$ si $_{0.2}$," *AIP Advances*, vol. 6, no. 11, p. 115104, 2016. [Online]. Available: http://aip.scitation.org/doi/10.1063/1.4967278

[5] A. Bravin, P. Coan, and P. Suortti, "X-ray phase-contrast imaging: from pre-clinical applications towards clinics," *Physics in Medicine and Biology*, vol. 58, no. 1, pp. R1–R35, dec 2012. [Online]. Available: https://doi.org/10.10882F0031-91552F582F12Fr1

[6] F. de Groot, "High-resolution x-ray emission and x-ray absorption spectroscopy," *Chemical Reviews*, vol. 101, no. 6, pp. 1779–1808, 2001, pMID: 11709999. [Online]. Available: https://doi.org/10.1021/cr9900681

[7] C. Watanabe, M. Ukibe, N. Zen, G. Fujii, K. Makise, M. Ohkubo, T. Lee, and D. Huang, "Development of superconducting nanostrip x-ray detector for high-resolution resonant inelastic soft x-ray scattering (rixs)," *IEEE Transactions on Applied Superconductivity*, vol. 29, no. 5, pp. 1–4, 2019.

[8] L. Ren, B. Zheng, and H. Liu, "Tutorial on x-ray photon counting detector characterization," *Journal of X-Ray Science and Technology*, vol. 26, pp. 1–28, 11 2017.

[9] A. Förster, S. Brandstetter, and C. Schulze-Briese, "Transforming x-ray detection with hybrid photon counting detectors," *Philosophical Transactions of the Royal Society A: Mathematical, Physical and Engineering Sciences*, vol. 377, no. 2147, p. 20180241, 2019. [Online]. Available: https://royalsocietypublishing.org/doi/abs/10.1098/rsta.2018.0241

[10] X. Liu, F. Grönberg, M. Sjölin, S. Karlsson, and M. Danielsson, "Count rate performance of a silicon-strip detector for photon-counting spectral ct," *Nuclear Instruments and Methods in Physics Research Section A: Accelerators, Spectrometers, Detectors and Associated Equipment*, vol. 827, pp. 102 – 106, 2016. [Online]. Available: http://www.sciencedirect.com/science/article/pii/S0168900216303047

[11] P. Trueb, B. A. Sobott, R. Schnyder, T. Loeliger, M. Schneebeli, M. Kobas, R. P. Rassool, D. J. Peake, and C. Broennimann, "Improved count rate corrections for highest data quality with PILATUS detectors," *Journal of Synchrotron Radiation*, vol. 19, no. 3, pp. 347–351, May 2012. [Online]. Available: https://doi.org/10.1107/S0909049512003950

[12] Jin Zhang, W. Slysz, A. Verevkin, O. Okunev, G. Chulkova, A. Korneev, A. Lipatov, G. Gol'tsman, and R. Sobolewski, "Response time characterization of NbN superconducting single-photon detectors," *IEEE Transactions on Appiled Superconductivity*, vol. 13, no. 2, pp. 180–183, Jun. 2003. [Online]. Available: http://ieeexplore.ieee.org/document/1211571/

[13] A. Gabutti, R. Wagner, K. Gray, R. Kampwirth, and R. Ono, "Superconducting detector for minimum ionizing particles," *Nuclear Instruments and Methods in Physics Research Section A: Accelerators, Spectrometers, Detectors and Associated Equipment*, vol. 278, no. 2, pp. 425–430, 1989. [Online]. Available: https://linkinghub.elsevier.com/retrieve/pii/0168900289908607

[14] A. Gabutti, K. Gray, R. Wagner, and R. Ono, "Granular-aluminum superconducting detector for 6 keV x-rays and 2.2 MeV beta sources," *Nuclear Instruments and Methods in Physics Research Section A: Accelerators, Spectrometers, Detectors and Associated Equipment*, vol. 289, no. 1, pp. 274–282, 1990. [Online]. Available: https://linkinghub.elsevier.com/retrieve/pii/016890029090270G

[15] A. Gabutti, K. Gray, G. Pugh, and R. Tiberio, "A fast, self-recovering superconducting strip particle detector made with granular tungsten," *Nuclear Instruments and Methods in Physics Research Section A: Accelerators, Spectrometers, Detectors and Associated Equipment*, vol. 312, no. 3, pp. 475–482, 1992. [Online]. Available: https://linkinghub.elsevier.com/retrieve/pii/016890029290197C

[16] L. Parlato, G. Peluso, G. Pepe, R. Vaglio, C. Attanasio, A. Ruosi, S. Barbanera, M. Cirillo, and R. Leoni, "X-rays operation of a thin film NbVN superconducting-strip particle detector," *Nuclear Instruments and Methods in Physics Research Section A: Accelerators, Spectrometers, Detectors and Associated Equipment*, vol. 348, no. 1, pp. 127–130, 1994. [Online]. Available: https://linkinghub.elsevier.com/retrieve/pii/0168900294908508

[17] D. Perez de Lara, M. Ejrnaes, A. Casaburi, M. Lisitskiy, R. Cristiano, S. Pagano, A. Gaggero, R. Leoni, G. Golt'sman, and B. Voronov, "Feasibility investigation of NbN nanowires as detector in time-of-flight mass spectrometers for macromolecules of interest in biology (proteins)," *Journal of Low Temperature Physics*, vol. 151, no. 3, pp. 771–776, 2008. [Online]. Available: http://link.springer.com/10.1007/s10909-008-9745-2

[18] K. Inderbitzin, A. Engel, A. Schilling, K. Il'in, and M. Siegel, "An ultra-fast superconducting nb nanowire single-photon detector for soft x-rays," *Applied Physics Letters*, vol. 101, no. 16, p. 162601, 2012. [Online]. Available: http://aip.scitation.org/doi/10.1063/1.4759046

[19] K. Inderbitzin, A. Engel, and A. Schilling, "Soft x-ray single-photon detection with superconducting tantalum nitride and niobium nanowires," *IEEE Transactions on Applied Superconductivity*, vol. 23, no. 3, pp. 2 200 505–2 200 505, 2013. [Online]. Available: http://ieeexplore.ieee.org/document/6384686/

[20] J. Zichi, J. Chang, S. Steinhauer, K. von Fieandt, J. W. N. Los, G. Visser, N. Kalhor, T. Lettner, A. W. Elshaari, I. E. Zadeh, and V. Zwiller, "Optimizing the stoichiometry of ultrathin NbTiN films for high-performance superconducting nanowire single-photon detectors," *Optics Express*, vol. 27, no. 19, p. 26579, 2019. [Online]. Available: https://www.osapublishing.org/abstract.cfm?URI=oe-27-19-26579

[21] C. Schuck, W. H. P. Pernice, and H. X. Tang, "Waveguide integrated low noise NbTiN nanowire single-photon detectors with milli-Hz dark count rate," *Sci Rep*, vol. 3, no. 1, p. 1893, Dec. 2013. [Online]. Available: http://www.nature.com/articles/srep01893

[22] S. Steinhauer, L. Yang, S. Gyger, T. Lettner, C. Errando-Herranz, K. D. Jöns, M. A. Baghban, K. Gallo, J. Zichi, and V. Zwiller, "NbTiN thin films for superconducting photon detectors on photonic and two-dimensional materials," *Applied Physics Letters*, vol. 116, no. 17, p. 171101, 2020. [Online]. Available: https://doi.org/10.1063/1.5143986

[23] P. J. Alonso, L. E. Halliburton, E. E. Kohnke, and R. B. Bossoli, "X-ray-induced luminescence in crystalline SiO $_2$," *Journal of Applied Physics*, vol. 54, no. 9, pp. 5369–5375, 1983. [Online]. Available: http://aip.scitation.org/doi/10.1063/1.332715

[24] A. A. Atta, A. M. Hassanien, M. M. El-Nahass, A. A. Shaltout, Y. A. Al-Talhi, and A. M. Aljoudi, "Influence of argon flow rate on structural and optical properties of transparent nb2o5 thin films," *Optical and Quantum Electronics*, vol. 51, no. 10, p. 341, 2019. [Online]. Available: http://link.springer.com/10.1007/s11082-019-2054-y

[25] A. J. Kerman, E. A. Dauler, W. E. Keicher, J. K. W. Yang, K. K. Berggren, G. Gol'tsman, and B. Voronov, "Kinetic-inductance-limited reset time of superconducting nanowire photon counters," *Applied Physics Letters*, vol. 88, no. 11, p. 111116, Mar. 2006. [Online]. Available: http://aip.scitation.org/doi/10.1063/1.2183810

[26] I. E. Zadeh, J. W. N. Los, R. B. M. Gourgues, G. Bulgarini, S. M. Dobrovolskiy, V. Zwiller, and S. N. Dorenbos, "A single-photon detector with high efficiency and sub-10ps time resolution," *arXiv:1801.06574 [physics]*, 2018. [Online]. Available: http://arxiv.org/abs/1801.06574